


Breast Tumor Cells Highly Resistant to Drugs Are Controlled Only by the Immune Response Induced in an Immunocompetent Mouse Model

Integrative Cancer Therapies
Volume 18: 1–16
© The Author(s) 2019
Article reuse guidelines:
sagepub.com/journals-permissions
DOI: 10.1177/1534735419848047
journals.sagepub.com/home/ict


Paola Lasso, PhD^{1,*}, Mónica Llano Murcia, MSc^{1,*}, Tito Alejandro Sandoval, PhD¹,
Claudia Urueña, PhD¹, Alfonso Barreto, PhD¹, and Susana Fiorentino, PhD¹ 

Abstract

Background: The tumor cells responsible for metastasis are highly resistant to chemotherapy and have characteristics of stem cells, with a high capacity for self-regeneration and the use of detoxifying mechanisms that participate in drug resistance. In vivo models of highly resistant cells allow us to evaluate the real impact of the immune response in the control of cancer. **Materials and Methods:** A tumor population derived from the 4T1 breast cancer cell line that was stable in vitro and highly aggressive in vivo was obtained, characterized, and determined to exhibit cancer stem cell (CSC) phenotypes (CD44⁺, CD24⁺, ALDH⁺, Oct4⁺, Nanog⁺, Sox2⁺, and high self-renewal capacity). Orthotopic transplantation of these cells allowed us to evaluate their in vivo susceptibility to chemo and immune responses induced after vaccination. **Results:** The immune response induced after vaccination with tumor cells treated with doxorubicin decreased the formation of tumors and macrometastasis in this model, which allowed us to confirm the immune response relevance in the control of highly chemotherapy-resistant ALDH⁺ CSCs in an aggressive tumor model in immunocompetent animals. **Conclusions:** The antitumor immune response was the main element capable of controlling tumor progression as well as metastasis in a highly chemotherapy-resistant aggressive breast cancer model.

Keywords

cancer stem cells, breast cancer, drug resistance, efflux pumps, ALDH, immune response

Submitted October 18, 2018; Revised March 26, 2019; accepted March 31, 2019

Introduction

Breast cancer tumor cells in mice are susceptible to treatment with drugs and to natural products obtained from *Caesalpinia spinosa* and others, as previously shown,¹⁻³ acting not only against the primary tumor but also against metastatic cells.⁴⁻⁶ One of the mechanisms involved in the antitumor activity of some of these therapies is the induction of immunogenic cell death, which is shared with certain chemotherapeutic drugs,⁷ inducing protective immune responses in melanoma and breast cancer mouse models.^{3,8} Although this antitumor activity reduces tumor size and metastasis, tumor cells are not completely eliminated, possibly because of the permanence of highly resistant tumor cells named cancer stem cells (CSCs).

CSCs comprise a tumor population capable of self-renewal and differentiation into other tumor populations.⁹

These cells were initially reported in 1994 by Lapidot and coworkers in an acute myeloid leukemia model,¹⁰ and almost 10 years later, CSCs were described in breast cancer.¹¹ CSCs are responsible for metastasis and relapse, in part because of their multidrug resistance (MDR) to conventional therapy,⁹ their expression of efflux pumps, DNA repair or detoxifying enzymes, and their high metabolic flexibility, among other factors, which allow CSCs to live in

¹Pontificia Universidad Javeriana, Bogotá, Colombia

*These authors contributed equally to this work.

Corresponding Author:

Susana Fiorentino, Grupo de Inmunobiología y Biología Celular,
Pontificia Universidad Javeriana, Carrera 7a. No. 43-82, Ed. 50, Lab. 101,
Bogotá C.P. 110211, Colombia.
Email: susana.fiorentino@javeriana.edu.co



highly hostile microenvironments. These factors may be intrinsic (independent of chemotherapy) or acquired (after being exposed to chemotherapy).¹²

Aldehyde dehydrogenase (ALDH) is one of the most important resistance mechanisms in CSCs and is known to decrease oxidative stress, particularly that caused by aldehydes.¹³ It has been shown that ALDH^{high} tumor cells are more resistant to treatment with radiation and certain drugs, such as gentamycin, carboplatin, etoposide, paclitaxel, and cyclophosphamide,¹⁴ and ALDH expression was recently reported to be a marker in the drug resistance profile of human CSC breast cancer cells.¹⁵ Additionally, ALDH^{high} CSCs seem to be involved in invasive and metastatic behavior in inflammatory breast cancer, and their presence in the tumor tissue of patients is a prognostic marker to predict metastasis and poor patient outcomes.¹⁶ All of these characteristics designate the CSC population as an important therapeutic target for treating cancer, and more recently, targeted therapies to activate the adaptive immune response against CSCs have been developed.¹⁷ However, to date, most CSC studies have been performed with human tumor-derived CSCs in nonobese diabetic/severe combined immunodeficiency (NOD/SCID) mice. The lack of an intact host immune system prevents the evaluation of multiple interactions that occur, such as epitope spreading, antigen cross-presentation, and immune evasion mechanisms involving T regulatory cells or myeloid-derived suppressor cells.¹⁸ A recent study showed that the immune response induced by autologous dendritic cells primed with breast cancer stem cells (BCSCs) significantly inhibited BCSC proliferation in vitro and decreased tumor size to a small degree by treating mice transplanted with BCSCs enriched with a verapamil-resistant screening method, which were confirmed by ALDH expression analysis and a mammosphere assay.¹⁹

All these studies show the role that the immune response can play in the elimination of this population. Despite this evidence, there are currently no animal models that allow progress in this field. In vitro protocols, such as 3D cultures or side population sorting, which attempt to enrich CSCs,^{20,21} do not accurately reproduce the true sensitivity or resistance that may occur in vivo or the interaction between these cells and the tumor microenvironment. To address this issue, we evaluated the in vitro and in vivo sensitivity of highly aggressive tumor cells exhibiting a stable positive ALDH phenotype²² to treatment with the standardized extract P2Et as well as in response to immunotherapy. We observed that vaccinated mice with doxorubicin-treated 4T1 H17 cells had fewer tumors and macrometastases than drug- or natural product-treated mice, and we found the presence of cytotoxic cells capable of lysing both the 4T1 parental cells and the CSC phenotype, providing evidence about the role of the immune response in the control of CSCs. Moreover, this model may allow the study of the impact of ALDH⁺ CSCs in the tumor microenvironment and tumor immune response modulation.

Materials and Methods

Natural Products

Caesalpinia spinosa pods were collected in Villa de Leyva, Boyacá, Colombia, and identified by Luis Carlos Jiménez at the Colombian National Herbarium (Voucher Specimen Number COL 523714, Colombian Environmental Ministry Agreement Number 220/2018 related to the use of genetic resources and derived products). The P2Et extract was obtained from *Caesalpinia spinosa* as previously described.²³

Animals

Female BALB/c mice (6-12 weeks old) were purchased from Charles River Laboratories International, Inc (Boston, MA) and housed in an animal research facility following the established protocols of the Ethics Committee of the Science Faculty and National and International Legislation for Live Animal Experimentation (Colombia Republic, Resolution 08430, 1993; National Academy of Sciences, 2010). Mice were housed in polyethylene cages with food and water provided ad libitum under a controlled temperature with a 12-hour light/dark cycle. Before treatment, the mice were acclimated for 1 week under standard conditions. The Ethics Committee of the Science Faculty approved the format for animal use on May 18, 2012, and the number of animals for each experiment was calculated using previous data from pilot experiments to reach a statistical power of 90%.

Tumor Cell Line and Culture Conditions

Murine mammary carcinoma 4T1 is a tumor cell line that was isolated in 1978²⁴ and grows in BALB/c mice and in tissue cultures. This cell line is highly tumorigenic and can develop spontaneous metastasis to different sites, such as lung, brain, and bone. Due to their resistance to 6-thioguanine, metastatic tumor cells can be easily isolated from distant organs.^{25,26} The murine mammary carcinoma was provided by Dr Alexander Asea (Texas A&M Health Science Center College of Medicine, Temple, TX). Cells were cultured in RPMI-1640 media (Eurobio, Toulouse, France) supplemented with 10% heat-inactivated fetal bovine serum (FBS; Eurobio), 2 mM L-glutamine, 100 U/mL penicillin, 100 µg/mL streptomycin, 0.01 M HEPES buffer, and 1 mM sodium pyruvate (Eurobio) and incubated in a humidified environment at 37°C and 5% CO₂. Cells were grown until 75% confluency, passaged using trypsin/1X EDTA (Eurobio), washed with PBS and resuspended in supplemented RPMI-1640 media.

Metastatic Cell Recovery From BALB/c Mice Bearing 4T1 Tumors

Metastatic cells were obtained as reported by Pulaski,²⁷ with minor changes. BALB/c mice were inoculated with 1×10^4 cells into the fourth mammary fat pad, allowing

primary tumor development. Twenty-five days later, the mice were humanely euthanized by CO₂ inhalation. First, the primary tumor, lungs, and liver were resected. Subsequently, the organs and tumor were transferred to RPMI-1640 media (Eurobio) supplemented with 2% penicillin/streptomycin (Eurobio). Next, the tissues were sliced into small pieces and digested with 2.5 mL of type-IV collagenase (Gibco, Life Technologies, New York, NY) in RPMI-1640 media supplemented with 10 mM HEPES, 2.5% fetal bovine serum (FBS), 2% penicillin/streptomycin, 1 mM sodium pyruvate, and 2 mM L-glutamine (Eurobio); lung and liver digestion was carried out at 4°C for 90 minutes. Subsequently, the tissues were filtered by a 70 µm cell strainer and centrifuged for 5 minutes at 300g, and after the lysis of red blood cells, the cells were cultured in the presence of 6-thioguanine (Sigma-Aldrich, St. Louis, MO) to select metastatic tumor cells. Once colonies were observed, attached cells were recovered with 0.25% trypsin/0.02% EDTA (Eurobio), and then the cells were washed with supplemented RPMI media and transferred to T-25 culture flasks. Metastatic cells were obtained from at least 3 different mice during 3 serial in vivo passages.

Analysis of Phenotype and Sorting by Flow Cytometry

Metastatic tumor cells were stained with the anti-mouse Sca-1 PE antibody (eBioscience, San Diego, CA, #12-5981-82), and then, the cells were sorted using a FACS Aria II instrument (BD Immunocytometry Systems, San José, CA). The ALDEFUOR assay kit (Stem Cell Technologies, Vancouver, Canada) was used according to the manufacturer's recommendation. Anti-mouse CD44 APC (BD Biosciences, San José, CA, #559250), anti-mouse CD24 PerCP-Cy5.5 (BD Biosciences, #562360), and anti-mouse Sca-1 PE antibodies were used to evaluate the breast CSC phenotype. Finally, the results were analyzed using FlowJo software (Tree Star, Inc, Ashland, OR).

Mammosphere Formation Assay

Mammosphere culture was performed as described before,²⁸ with slight modifications. In brief, 3×10^3 cells were seeded into a 24-well plate with serum-free medium containing DMEM/F12 1:1 (Gibco), N2 supplement (Gibco), B27 without vitamin A (Gibco), 100 U/mL penicillin, and 100 µg/mL streptomycin (Eurobio) in ultralow attachment plates (Corning, New York, NY). Cells were treated every day for 6 days using sublethal concentrations. Finally, on the seventh day of culture, the mammospheres were collected, washed twice with PBS, and centrifuged at 100g for 5 minutes, and all the mammospheres with a diameter greater than 50 µm were counted under a microscope. The mammosphere area was calculated by AxioVision software

(Carl Zeiss, Thornwood, NY) calibrated with a microscopy calibration slide of 10 µm. Finally, the mammosphere forming efficiency (MFE) was calculated using the following formula: $MFE = (\# \text{ counted mammospheres} / \# \text{ seeded cells}) \times 100$.²⁹

Limiting Dilution Assay

From a stock solution of 40 cells in 12 mL of mammosphere medium, 100 µL was added per well into a 96-well ultralow attachment plate to culture 1 cell per every 3 wells. The plates were cultured, and after 7 days, the wells with only one sphere were counted; this assay was performed with 4T1 and 4T1 H17 cells.²²

Cytotoxicity Assay

The cytotoxicity of doxorubicin (MP Biomedicals, Solon, OH), either alone or in combination with the ALDH inhibitor DEAB, was determined by methylthiazol tetrazolium (MTT) assays (Sigma-Aldrich).³ The inhibitory concentration 50 (IC₅₀) was calculated using GraphPad Prism version 6.0 for Mac OS X statistics software (GraphPad Software, San Diego, CA).

4T1 Side Population Cell Generation

To obtain cells that overexpressed efflux pumps such as Pgp, 4T1 cells were treated with a sublethal concentration of doxorubicin for 1 month. Subsequently, the cells were stained with Hoechst dye, and the unstained population or "side population" was sorted on a BD FACS Aria II cytometer (BD Immunocytometry Systems). The side population fraction was always cultured in the presence of doxorubicin and was called the 4T1 side population (4T1 sp).

Drug Efflux Assay

Pgp drug efflux activity was measured using perchlorate of tetramethylrhodamine methyl ester (TMRM) based on the report by Minderman et al,³⁰ with minor modifications.²² A single-cell suspension was obtained via trypsin/EDTA treatment, and 2.5×10^5 cells were incubated in the absence or presence of cyclosporine A (CsA; Sigma-Aldrich) for 1 hour at 4°C. Then, 40 nM TMRM was added and incubated for 1 hour on ice. Next, the samples were incubated at 37°C for 3 hours for Pgp activation. After incubation, 2 mL of ice-cold PBS was added, and the samples were centrifuged for 5 minutes at 200g at 4°C, washed twice with cold PBS (2% FBS), and analyzed on a BD FACS Aria II cytometer (BD Immunocytometry Systems). The analyses were performed on viable cells selected using a LIVE/DEAD Fixable Aqua Dead Cell Stain Kit (Life Technologies).

RT-PCR of ABC Pumps and Transcription Factors

Total RNA of cells was extracted using TRIzol LS reagent according to the manufacturer's instructions (Life Technologies Corporation, Invitrogen, NY). RNA quality and quantity were assessed with a NanoDrop spectrophotometer (NanoDrop Technologies). cDNA was synthesized with SuperScript III Reverse Transcriptase (Invitrogen) following the manufacturer's instructions. For real-time PCR (polymerase chain reaction), 600 ng of cDNA, DNA Master Plus SYBR Green I (Roche Applied Science, Indianapolis, IN) and 250 nM forward and reverse primers were added in a total volume of 20 μ L. The following primers were used: Oct4 (forward: TGAAGCAGAAGAGGATCACC; reverse: CTGCAAGGCCTCGAAGC), Nanog (forward: GAAGACCTGCCTCTTCAAGG; reverse: CCGCATCTTCTGCTTCTG), and Sox2 (forward: GCAACGGCAGCTACAGCAT; reverse: TGCAGGGCGCTGACGTC). Reactions were performed in 2 independent experiments with duplicates using Spectrum 48 Real-Time Thermal Cyclers (ESCO). The thermal cycling conditions were as follows: an initial denaturation step at 95°C for 10 minutes, 40 cycles at 95°C for 10 seconds, 60°C for 10 seconds, and 72°C for 10 seconds, followed by a dissociation stage. The relative expression levels of the Oct4, Nanog, and Sox2 genes were normalized to the endogenous control gene GAPDH. Relative expression was calculated using the $2^{-\Delta\Delta CT}$ comparative method.³¹

In Vivo Effect of Doxorubicin and P2Et in the 4T1 H17 Model

A total of 1×10^4 4T1 H17 cells were orthotopically transplanted into BALB/c mice. After 5 days, the mice were treated with doxorubicin (1 mg/kg) once per week, P2Et (18.7 mg/kg) twice per week, or PBS (control group). Tumor growth was recorded thrice per week. Experiments were finished on day 21 when mice showed compromised health.

In Vivo Effect of Vaccination With Doxorubicin-Treated Cells

4T1 or 4T1 H17 cells were treated in vitro with doxorubicin for 48 hours as previously reported,² and when more than 80% of the cells were dead (assayed by trypan blue dye), 3×10^6 treated cells were injected subcutaneously into the fourth right mammary gland. Six days after vaccination, 1×10^4 4T1 or 4T1 H17 live cells were inoculated into the fourth left mammary gland (the opposite site), and after 5 days, the mice were treated with an adjuvant (SC) (90 mg/kg) twice per week. Nonvaccinated mice were orthotopically transplanted with live 4T1 or 4T1 H17 cells and treated with the adjuvant (SC) only for use as a positive tumor growth control or with PBS (negative control).

Evaluation of the Immune Response by Flow Cytometry

To evaluate the immune response of vaccinated mice, cells were obtained from the spleen, tumor-draining lymph nodes (TDLNs), and the tumor by mechanical or enzymatic cleavage. The cells were cultured with phorbol 12-myristate 13-acetate (PMA) and ionomycin (P/I) or without a stimulus (ex vivo) for 7 hours. The last 6 hours of culture were performed in the presence of brefeldin A (1 μ g/mL) (BD Pharmingen). Briefly, 1×10^6 cells were stained with a LIVE/DEAD Fixable Aqua Dead Cell Stain Kit (Life Technologies, Thermo Scientific, Eugene, OR) for 20 minutes in the dark at room temperature. After washing with PBS containing 2% FBS, the cells were stained for 30 minutes at 4°C in the dark with anti-CD3 Pacific Blue (BioLegend, San Diego, CA, #100214), anti-CD4 PerCP (BD Biosciences, #553052), anti-CD8 PE Texas Red (BioLegend, #100762), and anti-CD45 PE (BD Biosciences, #553081) antibodies. Later, the cells were washed, fixed, and permeabilized for final staining with anti-IFN γ Alexa Fluor 700 (BD Biosciences, #557998), TNF α PE-Cy7 (BD Biosciences, #557644), and IL-2 FITC (BD Biosciences, #554427) for 30 minutes at 4°C in the dark. Finally, the cells were washed and resuspended in 300 μ L of PBS containing 2% FBS. Cells were acquired through flow cytometry using a FACS Aria II instrument (BD Immunocytometry Systems) flow cytometer, and the results were subsequently analyzed using FlowJo software (Tree Star). Multifunctional analyses were performed using a Boolean gating strategy. The data are presented using Pestre version 1.7 and SPICE version 5.3 software (the National Institutes of Health, Bethesda, MD).³²

Cytotoxicity Assay by Flow Cytometry, CFSE/7-Amino Actinomycin D

To expand tumor-specific cytotoxic T cells, splenocytes (3×10^6) from vaccinated and nonvaccinated 4T1 or 4T1 H17 tumor-bearing mice were placed into each well of a 24-well culture plate with 3 mL of RPMI-1640 (Eurobio) supplemented with 10% FBS (Eurobio), 2 mM L-glutamine, 100 U/mL penicillin, 100 μ g/mL streptomycin, 0.01 M HEPES buffer, 1 mM sodium pyruvate (Eurobio), IL-2 (10 UI/mL), IL-7 (1 ng/mL), and 4T1 or 4T1 H17 cell lysate (20 μ g/mL) and incubated in a humidified environment at 37°C and 5% CO₂ for 4 days. Later, the cells were restimulated with the respective cell lysate (20 μ g/mL) and cultured for 3 additional days. Then, the cells were collected and resuspended in medium for the cytotoxicity assay. 4T1 or 4T1 H17 cells were labeled with carboxyfluorescein succinimidyl ester (CFSE; Thermo Fisher Scientific) at a final concentration of 1 μ M for 20 minutes at 37°C following the manufacturer's recommendations. After quenching, the labeling reaction was stopped by the addition of complete culture medium,

followed by a 5-minute incubation at 37°C. After 2 washes, the CFSE-labeled target cells were resuspended and used for the cytotoxicity assay. The cell concentration was adjusted to 5×10^5 cells/mL, and 100 μ L/well was plated into 96-well plates. Splenocytes were added at 10:1 and 20:1 effector-target (E:T) ratios. The plates were incubated in a humidified atmosphere of 5% CO₂ and 37°C. After 12 hours, the wells were harvested and labeled with 7-aminocinactinomycin D (7-AAD; BD Biosciences, #559925) to stain dead cells. All cells in each tube were acquired on a FACSAria II instrument (BD Immunocytometry Systems) flow cytometer, and the results were analyzed using FlowJo software (Tree Star). Analysis was performed by gating on the target cells and measuring the 7-AAD-positive cells.³³ Cells positive for both 7-AAD and CFSE were considered lysed. Additionally, we calculated the percentage of cell loss in each well assuming that the number of target cells read from the 0:1 effector-target ratio was 100% of events. This percentage was added to the percentage of dead cells, and the percentage of cytotoxic activity was calculated using the following equation:

$$\text{Cytotoxicity (\%)} = \frac{100 \times \left[\frac{\text{dead target cells (\%)} - \text{spontaneous death (\%)}}{100 - \text{spontaneous death (\%)}} \right]}{\left[100 - \text{spontaneous death (\%)} \right]}$$

Results

4T1 3D Culture Cell Line Increased ALDH Expression

The study of CSC biology requires the appropriate growth of cells. Thus, the 3D culture is an anchorage-independent culture that allows the growth of tumor cells that have overcome anchorage dependency for growth as CSCs. The cell line 4T1 was 3D cultured for 7 days in ultralow attachment plates and serum-free medium. Seven days after culture, the spheres were collected and disaggregated with trypsin to obtain a single-cell suspension. The cells were stained with CSC markers (ALDH, CD44, CD24, and Sca-1), and the results were assessed by flow cytometry. We observed no change in the expression of CD24 and CD44 among 2D or 3D cultures, and surprisingly, Sca-1 expression was diminished by 10% in the 3D culture. In contrast, ALDH expression was increased in cells that grew on 3D culture compared with those that grew on 2D culture (Figure 1A).

We were not expecting the Sca-1 diminution in the 3D culture, since Sca-1 has been reported as an important marker of CSC in some breast cancer models.^{34,36} Thus, to evaluate some of the differences between Sca-1⁺ and Sca-1⁻ cells, we sorted both populations from 4T1 cells cultured in 2D format (Figure 1B). Then, each population was cultured independently in ultralow attachment plates and serum-free medium for 7 days, and subsequently, the spheres were collected and

counted. Although no differences between the sphere diameters from 4T1 Sca-1⁺ and 4T1 Sca-1⁻ cells were found, the 4T1 Sca-1⁺ cells formed more spheres than their negative counterparts (Figure 1C), suggesting that the Sca-1 molecule plays an important role in sphere formation but not necessarily in maintaining them.

4T1 Metastatic Cells Were More Aggressive Than the Parental Cell Line

Given that CSCs may be enriched after multiple in vivo passages,³⁷ we decided to enrich these populations to study their biological characteristics. We recovered liver and lung tumor metastatic cells after the first orthotopic tumor transplantation and then we compared them with the WT 4T1 cell line in terms of the MFE and malignancy in vivo. Although the 4T1 cell line showed a higher MFE compared with 4T1 cells recovered from the liver and lung (Figure 1D), the mammosphere sizes of 4T1 cells from the lung and liver were larger than those from conventional 4T1 cells (Figure 1E). In addition, even though metastatic 4T1 lung cells produced smaller primary tumors than the parental 4T1 cells (Figure 1F), the mice died significantly earlier than their counterparts (Figure 1G), suggesting that these metastatic cells are more malignant than those in the conventional 4T1 cell line. Then, lung metastatic cells recovered after the first orthotopic tumor transplantation were implanted twice more, recovered again from the lung and named as 4T1 H17 cells.

4T1 H17 Cells Exhibited Characteristics of Cancer Stem Cells

CSCs of epithelial tumors exhibit phenotypic and morphological characteristics that allow their identification, including mesenchymal morphology, low growth rate, expression of CD44, CD24, and ALDH, a high in vitro MFE, and the overexpression of key transcription factors, such as Oct4, Nanog, and Sox2, for the maintenance of the stem cell phenotype.³⁸⁻⁴⁰ We found that 4T1 H17 cells exhibited morphological differences from the parental cell line, such as a mesenchymal-like morphology and lower cell number, after 24 hours of 2D culture (Figure 2A). Additionally, 4T1 H17 cells had a higher MFE in the 3D setup (Figure 2B), which was confirmed by a limiting dilution assay (Figure 2C), suggesting higher intrinsic autorenewal capacity together with a higher number of CSCs. Phenotypic analysis of 4T1 and 4T1 H17 cells showed no differences in CD24 and CD44 expression; nevertheless, a higher percentage of Sca-1⁺ cells was observed in 4T1 conventional cells (36.4%) compared with 4T1 H17 cells (10.7%). Indeed, the main difference was a 10-fold increase in the percentage of ALDH⁺ cells in 4T1 H17 cells compared with WT 4T1 cells

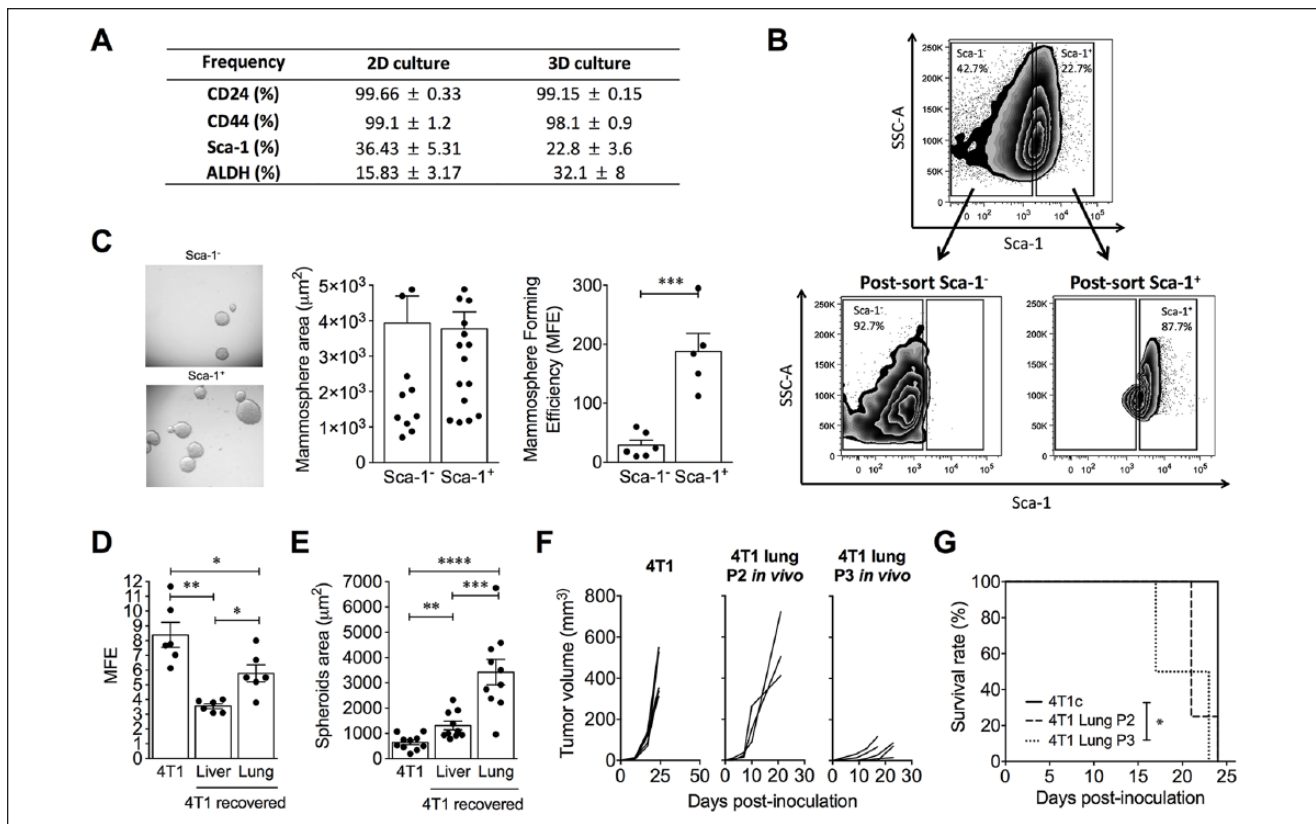


Figure 1. 4T1 3D culture increases the percentage of ALDH⁺ cells, although Sca-1 is important for mammosphere formation. (A) Frequency of cells expressing cancer stem cell markers (CD24, CD44, Sca-1, ALDH) on 4T1 cells grown in 2D and 3D cultures. (B) Representative flow cytometry plots showing the pre- and postsorting of Sca-1⁺ and Sca-1⁻ cells. (C) Representative image of mammosphere formation from Sca-1⁺ and Sca-1⁻ 4T1 cells. Bars show the mammosphere diameter (μm²) and mammosphere forming efficiency (MFE) of Sca-1⁺ and Sca-1⁻ 4T1 cells. (D) Mammosphere forming efficiency and (E) mammosphere diameter (μm²) of conventional 4T1 cells and metastatic 4T1 cells recovered from liver and lung. (F) Primary tumor growth in mice inoculated with conventional 4T1 and metastatic cells obtained from lung after serial passages in vivo. (G) Kaplan-Meier survival analysis in mice inoculated with conventional 4T1 and metastatic cells obtained from lung after serial passages in vivo. In all cases, data are presented as the mean ± SEM. The *P* values were calculated using the Mann-Whitney *U* test. **P* < .05, ***P* < .01, *****P* < .001.

(71.3% vs 7.5%, respectively; Figure 2D). The expression of ALDH remained stable throughout the time of the experiment, and we are currently able to maintain frozen stocks of the line, which do not lose their ALDH expression, even after thawing, and its expression is further enriched after new in vivo passages. Moreover, we observed that Oct4, Nanog, and Sox2 were overexpressed (4-fold) in 4T1 H17 cells (Figure 2E), showing that 4T1 H17 cells are enriched in cells with CSC characteristics.

4T1 H17 Exhibited Higher Drug Resistance due to ALDH Overexpression

Since CSCs show a highly drug-resistant phenotype,^{41,42} we compared the resistance factor to doxorubicin treatment between WT 4T1, 4T1 H17, and drug-resistant 4T1 cells previously obtained in our laboratory that overexpress P-glycoprotein (4T1 sp). It was found that 4T1 sp and 4T1

H17 cells were much more resistant (15- and 4-fold, respectively) than 4T1 WT cells (Figure 3A). Multidrug resistance can be due to multiple factors, among which is the overexpression of ABC pumps⁴³; thus, to test whether the resistance was due to ABC pump expression, MRP1, BCRP, and Pgp expression levels were evaluated by RT-PCR. Unexpectedly, 4T1 H17 cells expressed only the MRP1 transcript, whereas 4T1 sp (MRP1⁺, Pgp⁺, and BCRP⁺) and WT 4T1 (MRP1⁺ and BCRP⁺) cells expressed all three (Figure 3B and C). This lower expression seemed to be related to the low TMRM efflux observed in 4T1 H17 cells compared with WT 4T1 and 4T1 sp cells (Figure 3D).

To determine whether ALDH was involved in drug resistance in 4T1 H17 cells, as previously reported in other models,¹⁵ we inhibited the ALDH enzyme with the specific inhibitor N,N-diethylaminobenzaldehyde (DEAB) for 48 hours using a classical MTT assay. We observed that DEAB decreased the IC₅₀ of doxorubicin only 1.4 times for 4T1

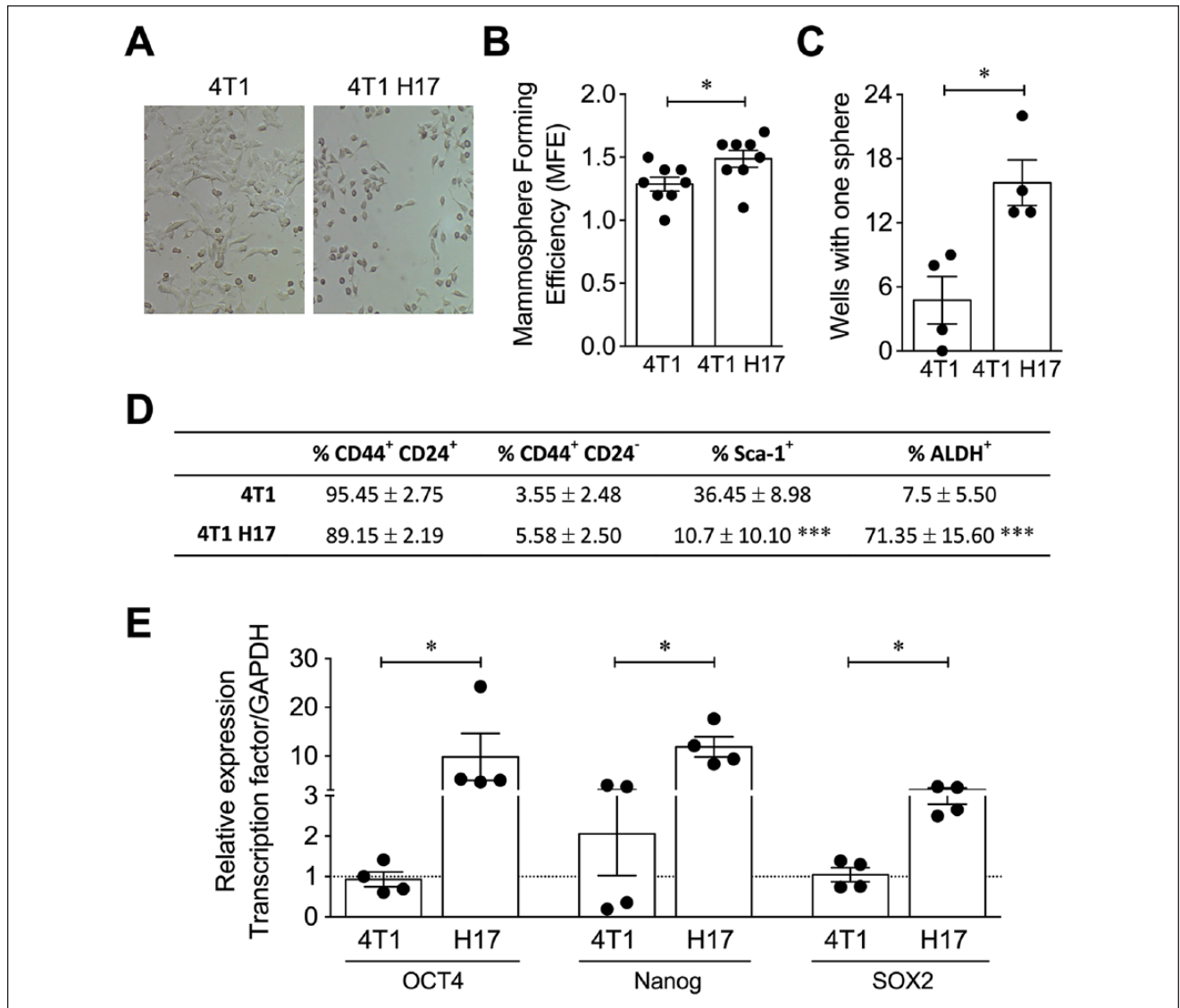


Figure 2. 4T1 H17 cells exhibited characteristics of cancer stem cells. (A) Representative image of conventional 4T1 and 4T1 H17 cells cultured in 2D. (B) Mammosphere forming efficiency of 4T1 and 4T1 H17 cells cultured for 7 days in ultralow attachment plates. (C) Sphere formation from single cells. 4T1 and 4T1 H17 cells were diluted to 1 cell per well in 96-well ultralow attachment plates, and sphere formation was tracked over time. After 7 days, the wells with only one sphere were counted. (D) Frequency of 4T1 and 4T1 H17 cells expressing cancer stem cell markers evaluated by flow cytometry. (E) Relative expression of the stem transcription factors Oct4, Nanog, and Sox2 by qRT-PCR in 4T1 and 4T1 H17 cells. In all cases, the data are presented as the mean ± SEM. The *P* values were calculated using the Mann-Whitney *U* test (B, C, E) and Student's *t* test (D). **P* < .05, ****P* < .001.

cells, while for 4T1 H17 cells, the reduction was 2.43 times (Figure 3E), suggesting that ALDH is involved in the drug resistance of 4T1 H17 cells.

4T1 H17 Was Highly Resistant to Treatments In Vivo

Previously, we reported that a sublethal concentration of doxorubicin and a mixture of polyphenols (P2Et) diminished the MFE of 4T1 H17 cells by 77% and 80%, respectively.²²

Based on these results and considering that the 3D culture models closely predicted the pharmaceutical response in vivo, we evaluated whether these treatments were effective in vivo. 4T1 H17 tumor cells were transplanted into BALB/c mice, and after 5 days of tumor implantation, mice were treated with 1 mg/kg of doxorubicin or 18.7 mg/kg of P2Et, as previously reported for the WT 4T1 cell line.³ Our results showed that neither doxorubicin nor P2Et reduced the tumor volume (Figure 4A and C) or weight (Figure 4B and D) and had an impact on the migration of tumor cells to the lung

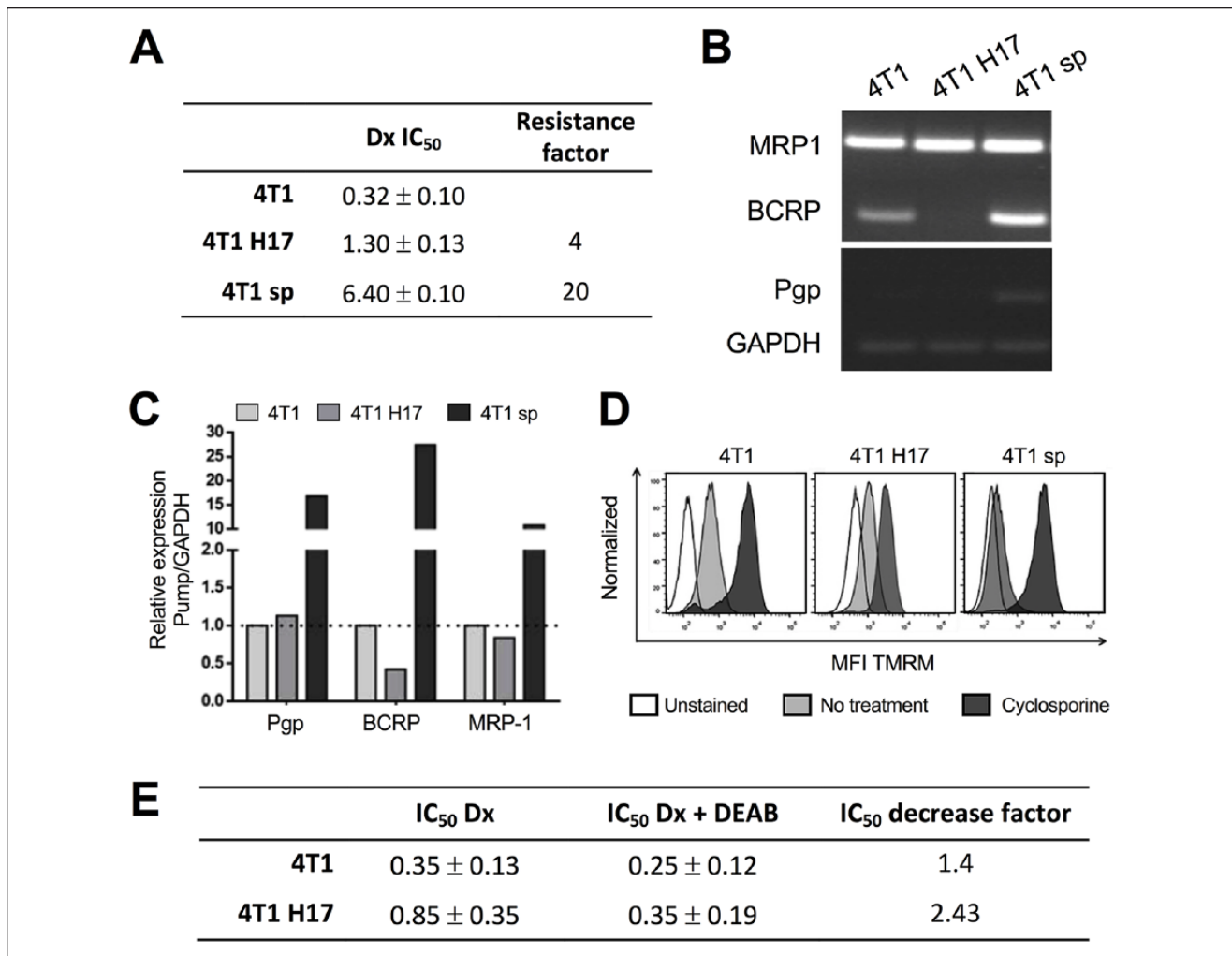


Figure 3. 4T1 H17 cells are more resistant to doxorubicin independent of ABC pump expression. (A) IC₅₀ values of 4T1, 4T1 H17, and 4T1 sp cells after treatment with doxorubicin (Dx). Total RNA was extracted from 4T1, 4T1 H17, and 4T1 sp cells to determine the mRNA expression of the ABC pumps by conventional (B) and real-time PCR (C). (D) 4T1, 4T1 H17, and 4T1 sp cells were cultured with or without cyclosporine A, and TMRM was subsequently added. Then, the MFI was analyzed by flow cytometry; histograms: white, unstained; light gray, no cyclosporine A treatment; and dark gray, cyclosporine A treatment. (E) IC₅₀ value in 4T1 and 4T1 H17 cells treated with Dx or Dx plus DEAB.

(Figure 4E). Additionally, metastatic tumor cells from the lung tissues of mice treated with doxorubicin and P2Et were principally ALDH⁺ cells (Figure 4F).

Induction of a Tumor-Specific Immune Response Could Decrease the Primary Tumor and Metastasis

An immune response to CSCs had been previously shown for head and neck squamous cell carcinoma, and specific CD8⁺ T cell responses were also identified in HLA-A2⁺ individuals with breast and pancreas carcinomas.⁴⁴ Additionally, we previously showed that vaccination with 4T1 tumor cells treated with P2Et or doxorubicin favored

the early generation of CD4⁺ and CD8⁺ T lymphocytes spontaneously producing IL-2 and TNF α after stimulation with 4T1 cells.² In this work, we examined the specific role of the immune response in the control of highly resistant 4T1 H17 tumor cells. After vaccination, we verified the expression of calreticulin on 4T1 H17 cells treated with doxorubicin or P2Et and found that doxorubicin induces higher expression of this protein on the plasma membrane (data not shown). Then, doxorubicin-treated 4T1 H17 cells were inoculated into the mammary gland of a group of mice, and after 5 days, untreated 4T1 H17 cells were inoculated into the opposite mammary gland. Five days later, the mice were treated with the adjuvant (SC) twice a week. Additionally, 2 control

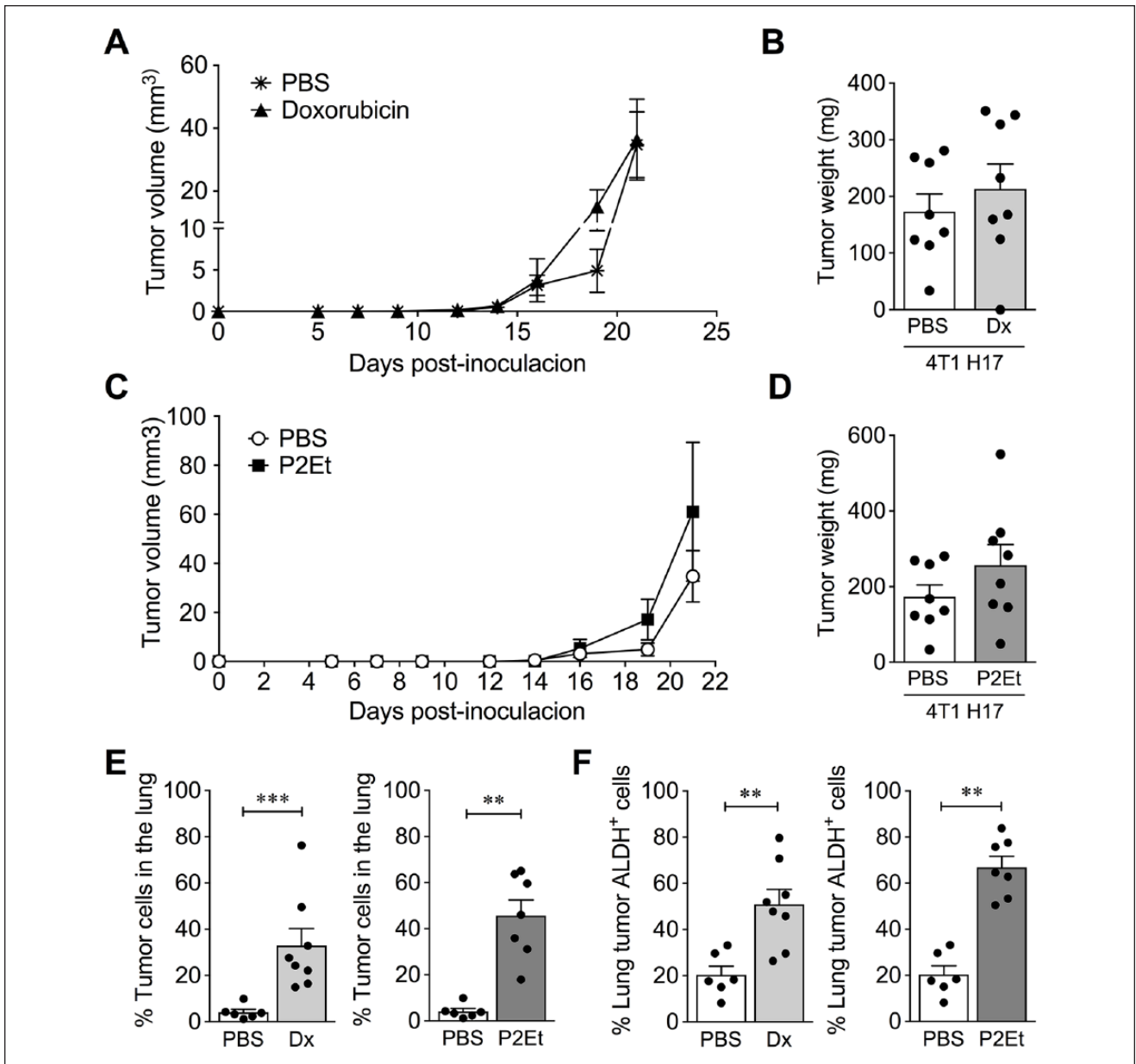


Figure 4. 4T1 H17 cells are resistant to doxorubicin and P2Et treatment in vivo. 4T1 H17 cells were inoculated into mouse mammary glands, which were then treated with PBS (control), Dx, or P2Et for 21 days. The tumors were measured and compared among groups. (A and C) Tumor volume (mm³) of 4T1 H17 control cells (PBS) versus 4T1 H17 cells treated with Dx or P2Et. (B and D) Tumor weight of 4T1 H17 control cells versus 4T1 H17 cells treated with Dx or P2Et. (E) Frequency of metastatic tumor cells in the lungs of mice bearing 4T1 H17 tumors treated with Dx or P2Et versus PBS. (F) The recovered cells of the lungs of mice bearing 4T1 H17 tumors treated with Dx or P2Et versus PBS. In all cases, data are presented as the mean \pm SEM. The *P* values were calculated using the Mann-Whitney *U* test. ***P* < .01, ****P* < .0001.

groups were inoculated with live cells only (nonvaccinated) and then treated with PBS or SC adjuvant (Figure 5A). By day 16, nonvaccinated controls started to show endpoint criteria such as weight loss, in contrast with vaccinated (Vax-SC) mice, which were not health compromised, and in whom smaller tumors were found (Figure

5B). Furthermore, only 5 of 8 vaccinated mice developed primary tumors (Figure 5C), and only 50% of mice developed macrometastasis compared with nonvaccinated mice, in which 7 of 8 developed distant macrometastasis (Figure 5D). The evaluation of affected organs showed that the control group had macrometastasis in the kidney

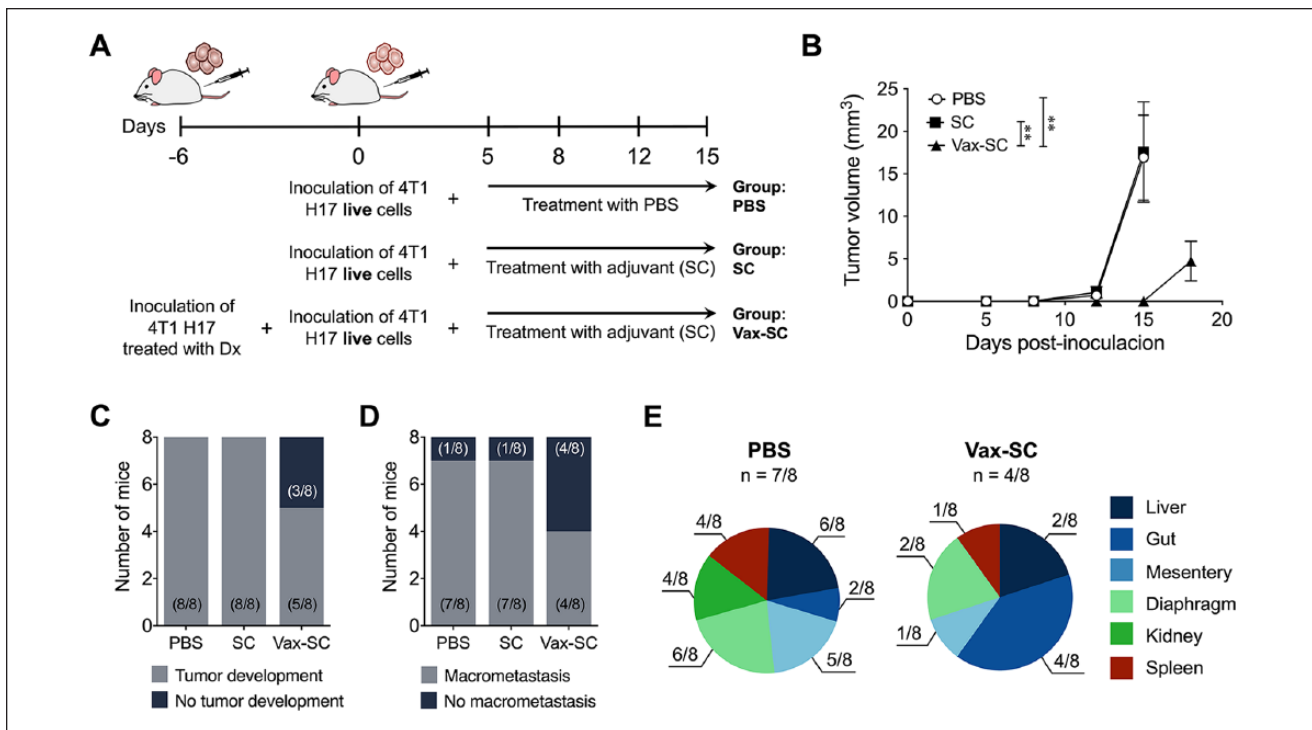


Figure 5. Mice vaccinated with 4T1 H17 cells treated with Dx showed a better outcome in the in vivo model. (A) Experimental treatment scheme. 4T1 H17 cells were treated for 48 hours with Dx and then inoculated into the mouse mammary gland; 6 days later, live cells were inoculated into the opposite mammary gland, and 5 days later, the mice were treated with 90 mg/kg of SC adjuvant twice a week. (B) Tumor volume (mm³) of the 4T1 H17 control (PBS) mice, 4T1 H17 mice treated with SC adjuvant (SC) or mice vaccinated with dead 4T1 H17 cells (Vax-SC) and then treated with SC adjuvant. (C) Pie charts showing the number of mice that developed tumors among the groups. (D) Pie charts showing the number of mice that developed macrometastasis among the groups. (E) Pie charts showing the different organs with macrometastasis and the number of mice that presented macrometastasis between groups. The *P* values were calculated using the Mann-Whitney *U* test. ***P* < .01.

(Figure 5E), diaphragm, and liver, while in vaccinated mice, the gut was the most affected organ (Figure 5E).

Functional Activity of T Cells From Vaccinated Mice

To evaluate the functional activity of CD4⁺ and CD8⁺ T cells, we measured IFN γ , TNF α , and IL-2 secretion in cells recovered from the spleen, TDLNs, and tumor. First, it was found that vaccinated mice had a higher number of CD3⁺, CD4⁺, and CD8⁺ cells in the spleen than the nonvaccinated mice (PBS; Figure 6A). Within this population, we observed a higher frequency of ex vivo CD4⁺ T cells producing TNF α , IFN γ , or IL-2 (Figure 6B) and a higher frequency of IFN γ or IL-2 CD4⁺ cells after in vitro stimulation with PMA/ionomycin on samples from vaccinated mice compared with nonvaccinated mice (Figure 6B). We also found that vaccinated mice had a higher frequency of mono- and polyfunctional CD4⁺ T cells compared with nonvaccinated mice both ex vivo and after stimulation with PMA/ionomycin (Figure 6C). Moreover, although no differences in the frequency or

number of intratumor CD45⁺ cells were found between the 2 groups of mice (data not shown), a higher frequency of recently activated intratumor CD4⁺ T cells secreting TNF α was evidenced in vaccinated mice (Figure 6D). The evaluation of these parameters in CD8⁺ T cells showed the same trend as for CD4⁺ T cells, namely, a higher frequency of CD8⁺ T cells producing cytokines ex vivo and after stimulation with PMA/ionomycin in vaccinated mice compared with nonvaccinated mice (Figure 6E), an increase in the frequency of mono- and polyfunctional CD8⁺ T cells ex vivo and after stimulation with PMA/ionomycin (Figure 6F), and an increase in recently activated intratumor CD8⁺ T cells producing TNF α (Figure 6G). Additionally, vaccination with doxorubicin-treated 4T1 H17 cells induced a higher frequency of cytotoxic cells against 4T1 H17 and conventional 4T1 tumor cells compared with nonvaccinated mice (Figure 7A and Supplemental Figure 1 [available online]). Moreover, following the same vaccination protocol with 4T1 cells, cytotoxic cells against 4T1 H17 cells were also generated (Figure 7B), suggesting that the immune response generated after the immunogenic cell death of conventional 4T1 cells can kill

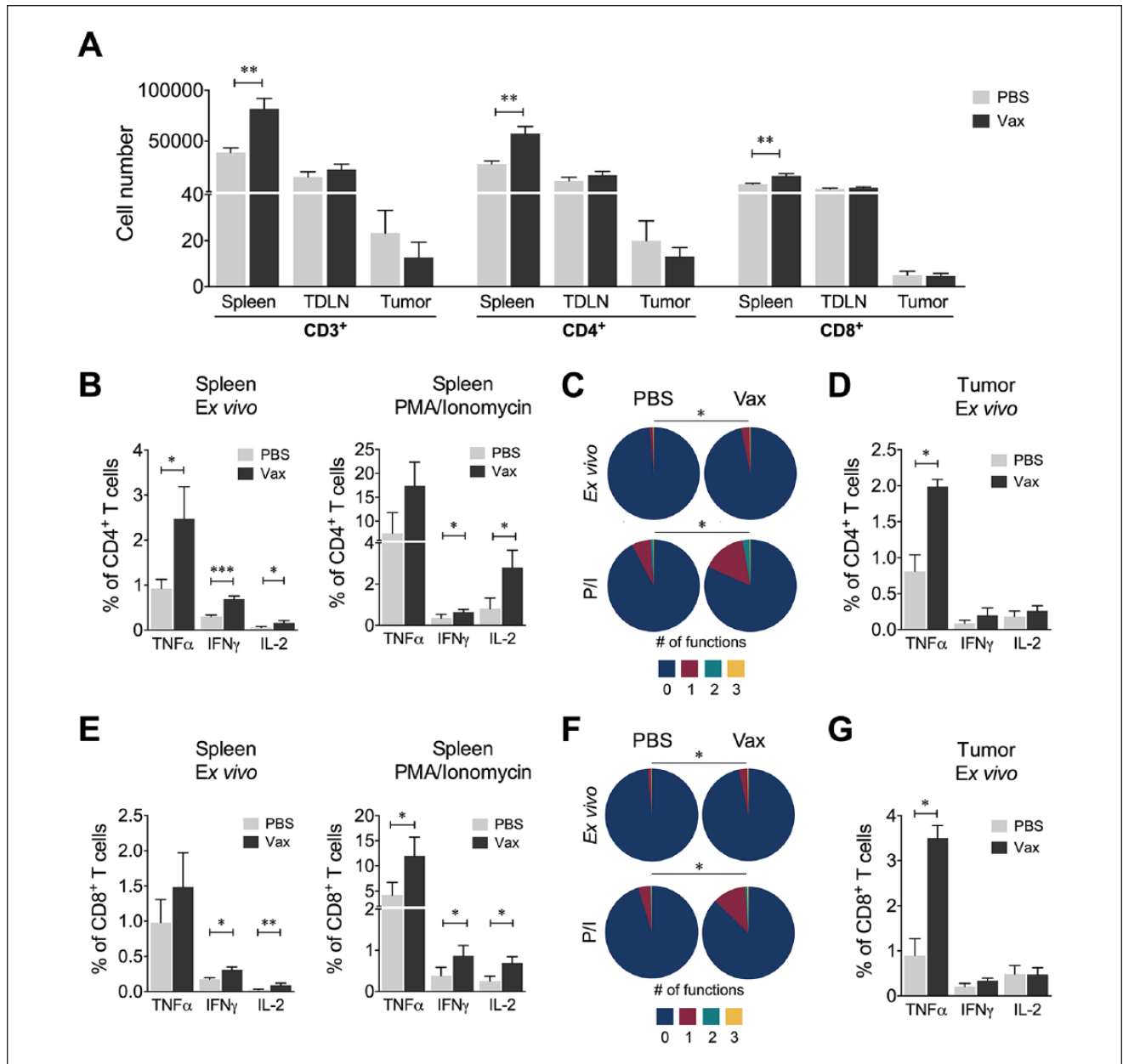


Figure 6. Immune response of T cells from vaccinated mice. (A) Number of CD3⁺, CD4⁺, and CD8⁺ T cells evaluated in the spleens, tumor-draining lymph nodes (TDLNs), and tumors from vaccinated (Vax) or nonvaccinated (PBS) mice. The number of cells reported in a tumor was determined as the cell number per mg of tumor. (B) Frequency of CD4⁺ T cells from spleen producing TNF α , IFN γ , or IL-2 ex vivo or following stimulation with PMA/ionomycin (P/I). (C) Polyfunctional activity of CD4⁺ T cells from spleen, without stimulus or following stimulation with P/I, from vaccinated or nonvaccinated mice. The functional profiles are grouped and color-coded according to the number of functions, as shown in the pie charts. (D) Frequency of CD4⁺ T cells from tumors producing TNF α , IFN γ , or IL-2 ex vivo or following stimulation with PMA/ionomycin (P/I). (E) Frequency of CD8⁺ T cells from spleen producing TNF α , IFN γ , or IL-2 ex vivo or following stimulation with P/I. (F) Polyfunctional activity of CD8⁺ T cells from spleen, without stimulus or following stimulation with P/I, from vaccinated or nonvaccinated mice. The functional profiles are grouped and color-coded according to the number of functions, as shown in the pie charts. (G) Frequency of CD8⁺ T cells from tumors producing TNF α , IFN γ , or IL-2 ex vivo or following stimulation with PMA/ionomycin (P/I). In all cases, the data are presented as the mean \pm SEM. The *P* values were calculated using the Mann-Whitney *U* test. The *P* values of the permutation test in the coexpression analysis (C and F) are shown in the pie charts. **P* < .05, ***P* < .01, ****P* < .001.

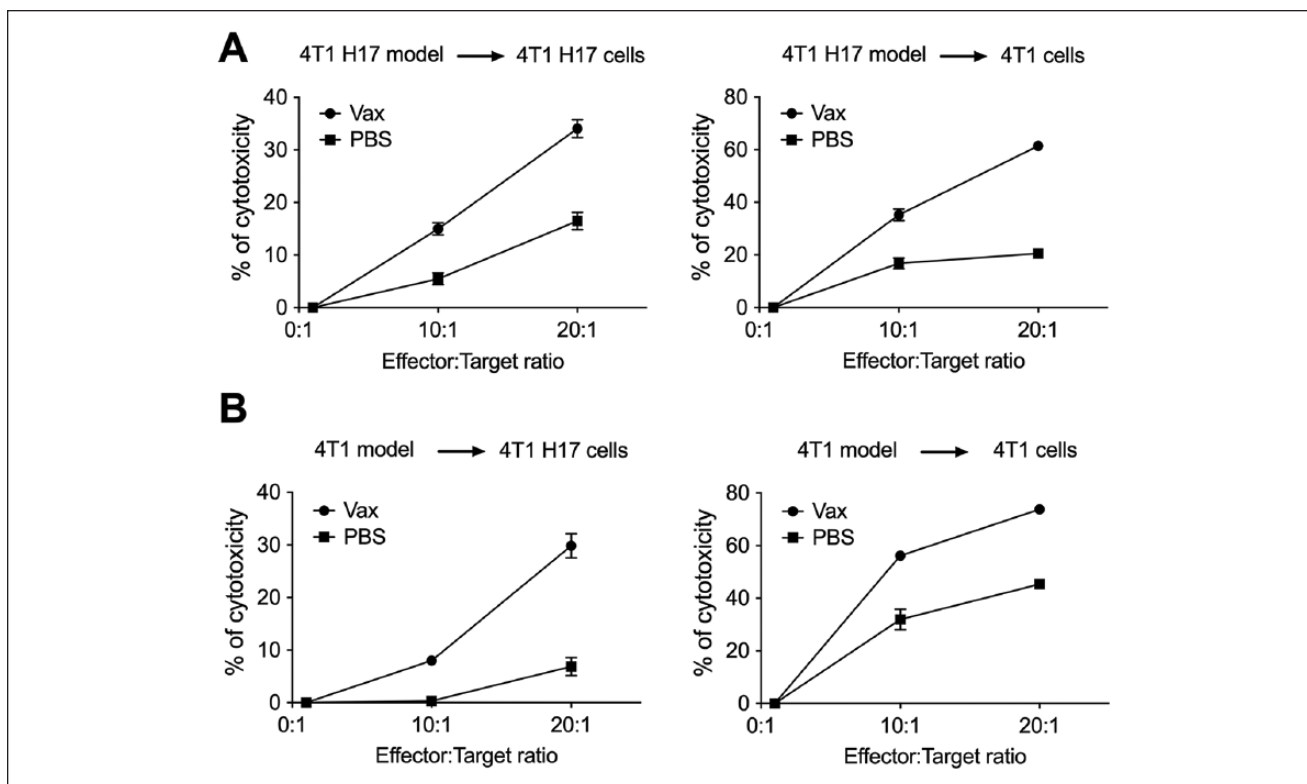


Figure 7. Cytotoxicity assay by CFSE and 7-AAD staining. CFSE-stained target cells were cocultured with spleen cells from vaccinated or nonvaccinated 4T1 or 4T1 H17 tumor-bearing mice at E:T ratios of 0:1, 10:1, and 20:1. (A) Cytotoxicity percentage of spleen cells from vaccinated or nonvaccinated 4T1 H17 tumor-bearing mice against 4T1 H17 or 4T1 conventional target cells. (B) Cytotoxicity percentage of spleen cells from vaccinated or nonvaccinated 4T1 tumor-bearing mice against 4T1 H17 or 4T1 conventional target cells. In all cases, the data are presented as the mean \pm SEM.

highly resistant CSCs, possibly because of the high number of shared antigens. These results highlight the importance of the induction of immunogenic death after first-line chemotherapy treatment for the control of metastases attributed to highly resistant tumor cells, which are subsequently enriched for therapy.

Discussion

The study of highly aggressive tumor models enriched in CSCs allows the search for new therapeutic strategies for breast cancer treatment. The majority of studies have isolated CSC populations by sorting them according to established surface markers or certain characteristics, such as dye expulsion.^{11,35,36} However, in the past, it has been shown that metastasis-recovered clones from 4T1-transplanted mice exhibit similar characteristics of CSCs, such as the formation of smaller tumors²⁶ and decreased survival.³⁷ In the present study, we found that the tumor cells recovered from lung metastasis formed fewer but larger mammospheres than the WT 4T1 cell line. Furthermore, after 3 serial *in vivo* passages, the cells showed a higher MFE than

WT 4T1 cells and exhibited a mesenchymal morphology; additionally, more than 70% of the cells expressed ALDH and had higher mRNA expression of transcription factors involved in multipotency maintenance, and the cells showed resistance to doxorubicin, as expected.⁴⁵ In addition, we found that the primary tumors of metastatic CSCs were smaller than those developed by the 4T1 cell line and that the mice died significantly earlier.

The resistance mechanism of 4T1 H17 cells is not mediated by ABC pump overexpression but seems to be due to the high frequency of ALDH⁺ cells. ALDH involvement as a drug resistance factor was discovered in a leukemic line and in hematopoietic progenitor cells overexpressing this enzyme, conferring resistance to cyclophosphamide *in vitro*.^{46,47} It was demonstrated that tissues from breast cancer patients without a response to chemotherapy overexpressed ALDH after treatment.⁴⁸ Additionally, sorted ALDH^{high} cells from the breast cancer cell lines MDA-MB-231 and MDA-MB-468 were more resistant to doxorubicin and Taxol than ALDH^{low} cells, and the inhibition of this enzyme diminished the resistance to these drugs.¹⁵ The mechanism of ALDH as a resistance factor in cancer cells is well

documented in the case of cyclophosphamide,⁴⁹ and for doxorubicin or Taxol it has been suggested that ALDH oxidizes highly toxic lipid-derived aldehydes produced by a high ROS concentration after chemotherapy treatment.⁵⁰

We previously showed that doxorubicin and a polyphenol mix (P2Et) are active in 2D and 3D 4T1 H17 cultures²² and demonstrated that P2Et is a fraction with potent antitumor activity in 2 mouse breast cancer models (4T1 and TS/a) and in a melanoma model (B16-F10).^{3,8,22} Unexpectedly, these treatments did not improve the outcome in mice bearing 4T1 H17 tumors in spite of our results from 3D cultures,²² contrary to the literature reports showing a correlation between 3D models and the *in vivo* response.²⁰ The tumor microenvironment is composed of different cells, such as immune cells, cancer-associated fibroblasts (CAFs), and endothelial cells, that could increase tumor cell drug resistance.⁵¹ In addition, we observed that doxorubicin- and P2Et-treated mice inoculated with 4T1 H17 cells showed more metastatic ALDH⁺ cells in the lung. In fact, previous reports have shown that neoadjuvant chemotherapy promotes the distant metastasis of breast cancer in mice and humans through a mechanism that favors CSC selection.⁵² In fact, the treatment of MDA-MB-231 cells with doxorubicin induces the production of transforming growth factor beta (TGF- β), which promotes epithelial-to-mesenchymal transition, causing migration to and invasion of distant organs.⁵³

P2Et is a standardized extract rich in polyphenols such as gallic acid and ethyl gallate and exhibits very high antioxidant capacity.²² Although there are several reports that show the beneficial effect of antioxidants, here, we showed that in our model enriched in CSCs, the treatment is not beneficial; in this sense, in 2014 and 2015, Martin Bergo's group showed that the supplementation of a mouse diet with antioxidants worsened lung and melanoma progression.^{54,55} In addition, a report in 1995 showed that the treatment of MCF7 tumor cells with a phenolic antioxidant increased the expression of ALDH.⁵⁶ We recently showed that although P2Et induced immunogenic cell death and considerably reduced the tumor size of both melanoma and breast cancer, the preconditioning of the host immune system with the P2Et extract did not involve a protective effect against the control of tumor growth and metastasis in these transplantable models, but in contrast, a detrimental effect was observed. We further demonstrated that this effect was partly due to an increase in regulatory T cells, myeloid-derived suppressor cells, and proinflammatory cytokines in healthy mice, with a concomitant decrease in CD4⁺ and CD8⁺ T cells.⁵⁷ All these results led us to believe that the presence of the tumor is fundamental to ensure the beneficial role of antioxidants such as P2Et and that the effective participation of the immune response in the control of highly aggressive tumors is fundamental for the control of the disease, as we show in this work.

In fact, immunotherapy is now a therapeutic option for cancer disease.⁵⁸ Recently, with the description of the CSC

population, some research groups have developed dendritic cell vaccines pulsed with CSC antigens such as ALDH and have shown promising results.^{18,59,60} Although we did not use dendritic cells pulsed with an antigen vaccine, we treated 4T1 H17 cells with doxorubicin, a well-known immunogenic cell death inducer in tumor cells,^{61,62} and observed that fewer mice developed primary tumors and macrometastases. In addition, their wellness was not compromised, suggesting that this treatment improved the control of the highly metastatic and resistant model 4T1 H17 cells. Additionally, we found that vaccination induced a response of CD4⁺ and CD8⁺ T cells through the individual production of cytokines and, furthermore, enhanced the polyfunctional activity of T cells. Although no differences in the frequency or number of intratumor CD4⁺ and CD8⁺ T cells were found between vaccinated and unvaccinated mice, a higher frequency of intratumor CD4⁺ and CD8⁺ T cells secreting TNF α was evidenced in vaccinated mice, showing that in this case, the quality of the response has greater importance. These results suggest that tumor growth control and the inhibition of metastasis development observed in vaccinated mice were, at least in part, due to an induction in the immune response. It has been reported that polyfunctional T cells, characterized by their ability to concomitantly produce 2 or more molecules, are more effective at controlling cancer.^{2,63-65} Thus, in this case, the only way to control our resistant model 4T1 H17 cells *in vivo* was the induction of a strong immune response with a high frequency of polyfunctional cells.

These results show that tumor diversity can be considered when an antitumor therapy is chosen. The findings highlight the fact that the use of combination therapies involving direct tumor-killing activity and immune activation may be more effective in the treatment of heterogeneous tumors than the use of therapies directed at a single molecular target.

Conclusions

Here, we obtained a CSC-enriched model by isolating metastatic tumor cells that were highly resistant to doxorubicin and polyphenol treatment from mouse lungs in several *in vivo* passages. Only the specific immune response evidenced on both secondary lymph organs and tumors improved the outcome of the mice, which showed a decrease in tumor and macrometastasis development.

Authors' Note

The datasets used and/or analyzed during the current study are available from the corresponding author on reasonable request.

Acknowledgments

The authors would like to thank Pontificia Universidad Javeriana for its support and the Colombian Environmental Ministry for allowing the use of genetic resources and derived products

(Agreement Number 0454 of 15/05/2013; Contract Number 60/2013). We also thank Paulo Rodriguez for his valuable technical advice.

Author Contributions

MLM, PL, and TAS: Design and execution of the experiments, acquisition and interpretation of data, and manuscript drafting (equal contributions). CU: Development of in vivo animal experiments and data acquisition and interpretation. AB: Data interpretation and analysis and manuscript drafting. SF: Leader of the project, design of the experiments, interpretation of the results, and manuscript revision.

Declaration of Conflicting Interests

The author(s) declared the following potential conflicts of interest with respect to the research, authorship, and/or publication of this article: SF, CU, and TAS are inventors of a granted patent related to P2Et. The rest of the authors declare no competing interests.

Ethics Approval

This project and the format using animals were approved by the Ethics Committee of the Science Faculty of Pontificia Universidad Javeriana, Bogotá, Colombia, on May 18, 2012.

Funding

The author(s) disclosed receipt of the following financial support for the research, authorship, and/or publication of this article: Funding was provided by the Departamento Administrativo de Ciencia, Tecnología e Innovación COLCIENCIAS (12011050101103) and Vicerrectoría de Investigaciones, Pontificia Universidad Javeriana (12081050401200), Bogotá, Colombia. Some of the experiments and fellowships of MLM, CU, and TAS were funded by the Sistema General de Regalías (BPIN: 2013000100196; Contract Number 1027-1-2015). PL was funded by the Departamento Administrativo de Ciencia, Tecnología e Innovación COLCIENCIAS (120356934596) and Vicerrectoría de Investigaciones, Pontificia Universidad Javeriana (DPS-05758-17), Bogotá, Colombia.

Supplemental Material

Supplemental material for this article is available online.

ORCID iD

Susana Fiorentino  <https://orcid.org/0000-0002-4664-0682>

References

- Bonofiglio D, Giordano C, De Amicis F, Lanzino M, Ando S. Natural products as promising antitumoral agents in breast cancer: mechanisms of action and molecular targets. *Mini Rev Med Chem*. 2016;16:596-604.
- Urueña C, Gomez A, Sandoval T, et al. Multifunctional T lymphocytes generated after therapy with an antitumor gallotannin-rich normalized fraction are related to primary tumor size reduction in a breast cancer model. *Integr Cancer Ther*. 2015;14:468-483.
- Urueña C, Mancipe J, Hernandez J, et al. Gallotannin-rich *Caesalpinia spinosa* fraction decreases the primary tumor and factors associated with poor prognosis in a murine breast cancer model. *BMC Complement Altern Med*. 2013;13:74.
- Kakarala M, Brenner DE, Korkaya H, et al. Targeting breast stem cells with the cancer preventive compounds curcumin and piperine. *Breast Cancer Res Treat*. 2010;122:777-785.
- Pandey PR, Okuda H, Watabe M, et al. Resveratrol suppresses growth of cancer stem-like cells by inhibiting fatty acid synthase. *Breast Cancer Res Treat*. 2011;130:387-398.
- Shankar S, Nall D, Tang SN, et al. Resveratrol inhibits pancreatic cancer stem cell characteristics in human and KrasG12D transgenic mice by inhibiting pluripotency maintaining factors and epithelial-mesenchymal transition. *PLoS One*. 2011;6:e16530.
- Mahbub AA, Le Maitre CL, Haywood-Small SL, Cross NA, Jordan-Mahy N. Polyphenols act synergistically with doxorubicin and etoposide in leukaemia cell lines. *Cell Death Discov*. 2015;1:15043.
- Gomez-Cadena A, Urueña C, Prieto K, et al. Immune-system-dependent anti-tumor activity of a plant-derived polyphenol rich fraction in a melanoma mouse model. *Cell Death Dis*. 2016;7:e2243.
- Nassar D, Blanpain C. Cancer stem cells: basic concepts and therapeutic implications. *Annu Rev Pathol*. 2016;11:47-76.
- Lapidot T, Sirard C, Vormoor J, et al. A cell initiating human acute myeloid leukaemia after transplantation into SCID mice. *Nature*. 1994;367:645-648.
- Al-Hajj M, Wicha MS, Benito-Hernandez A, Morrison SJ, Clarke MF. Prospective identification of tumorigenic breast cancer cells. *Proc Natl Acad Sci U S A*. 2003;100:3983-3988.
- Holohan C, Van Schaeybroeck S, Longley DB, Johnston PG. Cancer drug resistance: an evolving paradigm. *Nat Rev Cancer*. 2013;13:714-726.
- Vasilou V, Pappa A, Estey T. Role of human aldehyde dehydrogenases in endobiotic and xenobiotic metabolism. *Drug Metab Rev*. 2004;36:279-299.
- Cojoc M, Mabert K, Muders MH, Dubrovska A. A role for cancer stem cells in therapy resistance: cellular and molecular mechanisms. *Semin Cancer Biol*. 2015;31:16-27.
- Croker AK, Allan AL. Inhibition of aldehyde dehydrogenase (ALDH) activity reduces chemotherapy and radiation resistance of stem-like ALDHhiCD44⁺ human breast cancer cells. *Breast Cancer Res Treat*. 2012;133:75-87.
- Charafe-Jauffret E, Ginestier C, Iovino F, et al. Aldehyde dehydrogenase 1-positive cancer stem cells mediate metastasis and poor clinical outcome in inflammatory breast cancer. *Clin Cancer Res*. 2010;16:45-55.
- Visus C, Wang Y, Lozano-Leon A, et al. Targeting ALDH (bright) human carcinoma-initiating cells with ALDH1A1-specific CD8⁺ T cells. *Clin Cancer Res*. 2011;17:6174-6184.
- Pan Q, Li Q, Liu S, et al. Concise review: targeting cancer stem cells using immunologic approaches. *Stem Cells*. 2015;33:2085-2092.
- Nguyen ST, Nguyen HL, Pham VQ, et al. Targeting specificity of dendritic cells on breast cancer stem cells: in vitro and in vivo evaluations. *Onco Targets Ther*. 2015;8:323-334.
- Edmondson R, Broglie JJ, Adcock AF, Yang L. Three-dimensional cell culture systems and their applications in

- drug discovery and cell-based biosensors. *Assay Drug Dev Technol.* 2014;12:207-218.
21. Lee J, Cuddihy MJ, Kotov NA. Three-dimensional cell culture matrices: state of the art. *Tissue Eng Part B Rev.* 2008;14:61-86.
 22. Sandoval TA, Urueña CP, Llano M, et al. Standardized extract from *Caesalpinia spinosa* is cytotoxic over cancer stem cells and enhance anticancer activity of doxorubicin. *Am J Chin Med.* 2016;44:1693-1717.
 23. Castañeda DM, Pombo LM, Urueña CP, Hernandez JF, Fiorentino S. A gallotannin-rich fraction from *Caesalpinia spinosa* (Molina) Kuntze displays cytotoxic activity and raises sensitivity to doxorubicin in a leukemia cell line. *BMC Complement Altern Med.* 2012;12:38.
 24. Dexter DL, Kowalski HM, Blazar BA, Fligiel Z, Vogel R, Heppner GH. Heterogeneity of tumor cells from a single mouse mammary tumor. *Cancer Res.* 1978;38:3174-3181.
 25. Pulaski BA, Ostrand-Rosenberg S. Reduction of established spontaneous mammary carcinoma metastases following immunotherapy with major histocompatibility complex class II and B7.1 cell-based tumor vaccines. *Cancer Res.* 1998;58:1486-1493.
 26. Lelekakis M, Moseley JM, Martin TJ, et al. A novel orthotopic model of breast cancer metastasis to bone. *Clin Exp Metastasis.* 1999;17:163-170.
 27. Pulaski BA, Ostrand-Rosenberg S. Mouse 4T1 breast tumor model. In: *Current Protocols in Immunology* (Chapter 20, Unit 20.2). New York, NY: John Wiley.
 28. Chen D, Pamu S, Cui Q, Chan TH, Dou QP. Novel epigallocatechin gallate (EGCG) analogs activate AMP-activated protein kinase pathway and target cancer stem cells. *Bioorg Med Chem.* 2012;20:3031-3037.
 29. Lombardo Y, de Giorgio A, Coombes CR, Stebbing J, Castellano L. Mammosphere formation assay from human breast cancer tissues and cell lines. *J Vis Exp.* 2015;(97). doi:10.3791/52671
 30. Minderman H, Suvannasankha A, O'Loughlin KL, et al. Flow cytometric analysis of breast cancer resistance protein expression and function. *Cytometry.* 2002;48:59-65.
 31. Schmittgen TD, Zakrajsek BA, Mills AG, Gorn V, Singer MJ, Reed MW. Quantitative reverse transcription-polymerase chain reaction to study mRNA decay: comparison of endpoint and real-time methods. *Anal Biochem.* 2000;285:194-204.
 32. Roederer M, Nozzi JL, Nason MC. SPICE: exploration and analysis of post-cytometric complex multivariate datasets. *Cytometry A.* 2011;79:167-174.
 33. Lecoeur H, Fevrier M, Garcia S, Rivière Y, Gougeon ML. A novel flow cytometric assay for quantitation and multiparametric characterization of cell-mediated cytotoxicity. *J Immunol Methods.* 2001;253:177-187.
 34. Grange C, Lanzardo S, Cavallo F, Camussi G, Bussolati B. Sca-1 identifies the tumor-initiating cells in mammary tumors of BALB-neuT transgenic mice. *Neoplasia.* 2008;10:1433-1443.
 35. Kruger JA, Kaplan CD, Luo Y, et al. Characterization of stem cell-like cancer cells in immune-competent mice. *Blood.* 2006;108:3906-3912.
 36. Liu JC, Deng T, Lehal RS, Kim J, Zacksenhaus E. Identification of tumorsphere- and tumor-initiating cells in HER2/Neu-induced mammary tumors. *Cancer Res.* 2007;67:8671-8681.
 37. Guo W, Zhang S, Liu S. Establishment of a novel orthotopic model of breast cancer metastasis to the lung. *Oncol Rep.* 2015;33:2992-2998.
 38. Chen K, Huang YH, Chen JL. Understanding and targeting cancer stem cells: therapeutic implications and challenges. *Acta Pharmacol Sin.* 2013;34:732-740.
 39. Visvader JE, Lindeman GJ. Cancer stem cells in solid tumours: accumulating evidence and unresolved questions. *Nat Rev Cancer.* 2008;8:755-768.
 40. Pattabiraman DR, Weinberg RA. Tackling the cancer stem cells—what challenges do they pose? *Nat Rev Drug Discov.* 2014;13:497-512.
 41. Clevers H. The cancer stem cell: premises, promises and challenges. *Nat Med.* 2011;(3):313-319.
 42. Moitra K, Lou H, Dean M. Multidrug efflux pumps and cancer stem cells: insights into multidrug resistance and therapeutic development. *Clin Pharmacol Ther.* 2011;89:491-502.
 43. Eckford PD, Sharom FJ. ABC efflux pump-based resistance to chemotherapy drugs. *Chem Rev.* 2009;109:2989-3011.
 44. Kwiatkowska-Borowczyk EP, Gabka-Buszek A, Jankowski J, Mackiewicz A. Immunotargeting of cancer stem cells. *Contemp Oncol (Pozn).* 2015;19(1A):A52-A59.
 45. Velasco-Velazquez MA, Homsí N, De La Fuente M, Pestell RG. Breast cancer stem cells. *Int J Biochem Cell Biol.* 2012;44:573-577.
 46. Magni M, Shammah S, Schiró R, Mellado W, Dalla-Favera R, Gianni AM. Induction of cyclophosphamide-resistance by aldehyde-dehydrogenase gene transfer. *Blood.* 1996;87:1097-1103.
 47. Hilton J. Role of aldehyde dehydrogenase in cyclophosphamide-resistant L1210 leukemia. *Cancer Res.* 1984;44:5156-5160.
 48. Tanei T, Morimoto K, Shimazu K, et al. Association of breast cancer stem cells identified by aldehyde dehydrogenase 1 expression with resistance to sequential paclitaxel and epirubicin-based chemotherapy for breast cancers. *Clin Cancer Res.* 2009;15:4234-4241.
 49. Emadi A, Jones RJ, Brodsky RA. Cyclophosphamide and cancer: golden anniversary. *Nat Rev Clin Oncol.* 2009;6:638-647.
 50. Kim J, Chen CH, Yang J, Mochly-Rosen D. Aldehyde dehydrogenase 2*2 knock-in mice show increased reactive oxygen species production in response to cisplatin treatment. *J Biomed Sci.* 2017;24:33.
 51. Hanahan D, Coussens LM. Accessories to the crime: functions of cells recruited to the tumor microenvironment. *Cancer Cell.* 2012;21:309-322.
 52. Karagiannis GS, Pastoriza JM, Wang Y, et al. Neoadjuvant chemotherapy induces breast cancer metastasis through a TMEM-mediated mechanism. *Sci Transl Med.* 2017;9:eaan0026.
 53. Bandyopadhyay A, Wang L, Agyin J, et al. Doxorubicin in combination with a small TGFbeta inhibitor: a potential novel therapy for metastatic breast cancer in mouse models. *PLoS One.* 2010;5:e10365.

54. Le Gal K, Ibrahim MX, Wiel C, et al. Antioxidants can increase melanoma metastasis in mice. *Sci Transl Med.* 2015; 7:308re8.
55. Sayin VI, Ibrahim MX, Larsson E, Nilsson JA, Lindahl P, Bergo MO. Antioxidants accelerate lung cancer progression in mice. *Sci Transl Med.* 2014;6:221ra15.
56. Sreerama L, Rekha GK, Sladek NE. Phenolic antioxidant-induced overexpression of class-3 aldehyde dehydrogenase and oxazaphosphorine-specific resistance. *Biochem Pharmacol.* 1995;49:669-675.
57. Lasso P, Gomez-Cadena A, Urueña C, et al. Prophylactic vs therapeutic treatment with P2Et polyphenol-rich extract has opposite effects on tumor growth. *Front Oncol.* 2018;8:356.
58. Dougan M, Dranoff G. Immune therapy for cancer. *Annu Rev Immunol.* 2009;27:83-117.
59. Ning N, Pan Q, Zheng F, et al. Cancer stem cell vaccination confers significant antitumor immunity. *Cancer Res.* 2012;72:1853-1864.
60. Pham PV, Le HT, Vu BT, et al. Targeting breast cancer stem cells by dendritic cell vaccination in humanized mice with breast tumor: preliminary results. *Onco Targets Ther.* 2016;9: 4441-4451.
61. Casares N, Pequignot MO, Tesniere A, et al. Caspase-dependent immunogenicity of doxorubicin-induced tumor cell death. *J Exp Med.* 2005;202:1691-1701.
62. Panaretakis T, Kepp O, Brockmeier U, et al. Mechanisms of pre-apoptotic calreticulin exposure in immunogenic cell death. *EMBO J.* 2009;28:578-590.
63. Ding ZC, Blazar BR, Mellor AL, Munn DH, Zhou G. Chemotherapy rescues tumor-driven aberrant CD4⁺ T-cell differentiation and restores an activated polyfunctional helper phenotype. *Blood.* 2010;115:2397-2406.
64. Lin Y, Gallardo HF, Ku GY, et al. Optimization and validation of a robust human T-cell culture method for monitoring phenotypic and polyfunctional antigen-specific CD4 and CD8 T-cell responses. *Cytotherapy.* 2009;11:912-922.
65. Yuan J, Gnjatic S, Li H, et al. CTLA-4 blockade enhances polyfunctional NY-ESO-1 specific T cell responses in metastatic melanoma patients with clinical benefit. *Proc Natl Acad Sci U S A.* 2008;105:20410-20415.